The electronic structure of 'linear' nickel oxides*

Adam J. Bridgeman

University Chemical Laboratories, Lensfield Road, Cambridge CB2 1EW, UK

The geometries, ground states and low-lying excited states of the 'linear' nickel oxides NiO, $[NiO_2]^{2-}$ and $[NiO_2]^{3-}$ have been studied using local density-functional (LDF) calculations within the linear combination of Gaussian-type orbitals framework. The NiO molecule and the $[NiO_2]^{2-}$ ion are predicted to have $^3\Sigma^-$ and $^3\Sigma_g^-$ ground states respectively. The calculated bond lengths and vibrational frequencies are in excellent agreement with experiment. Cellular ligand-field (CLF) analyses of the spectra and magnetic properties have also been performed. The LDF and CLF calculations provide a consistent description of the bonding and suggest that the oxide ions are acting as good σ and π donors in these molecules with both roles enhanced compared to systems with higher co-ordination numbers. The interaction between the d_σ orbital and the antibonding σ orbital of predominantly nickel s-orbital character is important in understanding the electronic structure of these systems and its modelling in CLF analyses is described. The description of the bonding in NiO is consistent with that obtained from previous studies. The prediction of a $^3\Sigma_g^-$ ground state for the $[NiO_2]^{2-}$ ion required a reassignment of the spectrum and led to a more satisfactory modelling of the magnetic moment than that given by earlier calculations. The ground state of the $[NiO_2]^{3-}$ ion is predicted to be $^2\Sigma_g^+$, consistent with its EPR spectrum. The bonding in this low-oxidation-state is weaker than in the nickel(II) oxides and involves considerable contributions from both nickel d and s orbitals.

The bonding in transition-metal oxides is generally taken to be highly ionic in character. There is a strong relationship between the co-ordination numbers adopted and the ionic radii of the metal and oxide ions.[1] The co-ordination number in transition-metal oxides is usually four or six with approximately tetrahedral or octahedral co-ordination respectively. Small distortions from ideal geometries are usually associated with the steric activity[2] of the metal d electrons, most typically due to a Jahn-Teller effect, or with metal–metal bonding. Larger distortions are found in certain complexes of d^0 metal ions. The complexes of the V^{5+} ion are often found to have one very short V–O bond length whilst Mo^{6+} complexes are found with two short Mo–O bonds. The metal–oxygen bond lengths in complexes containing VO^{3+} and MoO_2^{2+} groups suggest, at least, double bonds and that covalency is important in determining the structures. The present study is concerned with the bonding in the oxides M_2NiO_2 and M_3NiO_2 where M is an alkali metal. These compounds[3–6] are remarkable in that they contain the $[NiO_2]^{2-}$ and $[NiO_2]^{3-}$ ions respectively in which the nickel is co-ordinated by just two oxygens in an approximately linear arrangement. The +1 oxidation state of the nickel ion in $[NiO_2]^{3-}$ is also unusually low for a metal oxide. More typically, the π-donor property and electronegativity of oxygen is used to stabilize the higher oxidation states of nickel and of other elements. Nickel(I) compounds are extremely rare and are characterized by having π-acceptor ligands and are, in general, binuclear.

The electronic structure of linear transition-metal complexes have centred on the dihalides, either in the gas phase or isolated in matrices. The geometry and electronic structure of these systems have been the subject of considerable study and controversy.[7–15] The co-ordination geometry in the M_2NiO_2 and M_3NiO_2 oxides has been determined[3–6,16] by X-ray crystallography and the nickel is found to be, at least approximately, linearly co-ordinated. Linear transition-metal complexes represent the limiting case of a tetragonal compression of the ligand field. Qualitative crystal-field arguments and simple molecular orbital considerations suggest that the d orbitals in linear transition-metal complexes are split into three levels, σ_g^+, π_g and δ_g, with relative energies $d_\sigma > d_\pi > d_\delta$. The electronic and magnetic properties of the linear oxides have been investigated by Möller *et al.*[16] and Hitchman *et al.*[17] These workers also performed angular overlap model (AOM) calculations and assumed this d-orbital sequence in interpreting these properties. Recent calculations[12–15] on $CuCl_2$ and $NiCl_2$, however, predict $^2\Pi_g$ and $^3\Sigma_g^-$ ground terms respectively based on the reversal of the relative energy of d_σ and d_π. The purpose of the present study is to reinvestigate the bonding in these linear oxides and their spectral and magnetic properties using local density-functional (LDF) calculations within the linear combination of Gaussian-type orbitals (LCGTO) framework and cellular ligand-field (CLF) calculations.

To assist the description of the bonding in these linear oxides, the electronic structure of the NiO molecule is also investigated. The ground state of this system has been demonstrated to be $^3\Sigma^-$ by study of the electronic spectrum at high resolution[18,19] as well as by a number of theoretical studies.[20–24] The dominant configuration for this ground state is $\delta_g^4\sigma_g^{+2}\pi_g^3$ with d_σ *lower* in energy than d_π.

Computational Details

Local density functional calculations are becoming an increasingly popular method of studying the properties of transition-metal compounds.[25–28] The LDF calculations were performed using the DEFT code written by St-Amant[29] in the LCGTO framework. The calculations on the M_2NiO_2 and M_3NiO_2 compounds were performed on the $[NiO_2]^{2-}$ and $[NiO_2]^3$ anions to give a local view of the bonding in these non-metallic compounds. Three types of calculation have been completed differing in the treatment of the exchange and correlation interactions. The first, labelled VWN, used the Vosko–Wilk–Nusair local spin-density (LSD) approximation of the exchange-correlation potential.[30] The second, labelled BP, corrects the LSD expression using the Becke[31] non-local functional for exchange and the Perdew[32] non-local functional for correlation. In the third approach, labelled MIX, the non-local corrections are added perturbatively to the energy and energy gradients of the self-consistent local density. Any changes in the density due

---

* *Non-SI units employed:* eV ≈ 1.60×10^{-19} J, $\mu_B \approx 9.27 \times 10^{-24}$ J T^{-1}.

J. Chem. Soc., Dalton Trans., 1996, Pages 4555–4562

Table 1 Calculated and experimentally determined properties of the ground and the low-lying excited states of NiO

State	Configuration[a]		Energy/cm^{-1}	Bond length/Å	$\tilde{\nu}_{sym}$/cm^{-1}
$^3\Sigma^-$	$\cdots(8\sigma)^2(3\pi)^4(1\delta)^4(9\sigma)^2(4\pi)^2$	Calc. VWN	0	1.620	825
		BP		1.638	841
		MIX		1.648	820
		Exptl. (*a*)	0	1.631	828
		(*b*)		1.626	828
$^3\Pi$	$\cdots(8\sigma)^2(3\pi)^4(1\delta)^4(9\sigma)^1(4\pi)^3$	Calc. VWN	4 000	1.650	790
		Exptl. (*b*)	4 293	1.644	769
$^3\Phi$	$\cdots(8\sigma)^2(3\pi)^4(1\delta)^3(9\sigma)^2(4\pi)^3$	Calc. VWN	6 200	1.683	755
$^3\Sigma^-$	$\cdots(8\sigma)^2(3\pi)^4(1\delta)^4(9\sigma)^1(4\pi)^2(10\sigma)^1$	Calc. VWN	14 200	1.690	750
		Exptl. (*b*)	16 000		
$^1\Delta$	$\cdots(8\sigma)^2(3\pi)^4(1\delta)^4(9\sigma)^2(4\pi)^2$	Calc. VWN	12 500	1.610	840

[a] The calculated frequencies and the experimental values are all for the ^{58}Ni^{16}O isotope. The configurations give only an approximate description of the state and give the electron arrangement outside the core (Ni $1s^22s^22p^63s^23p^6$ and O $1s^22s^2$) electrons. The experimental values are from (*a*) analysis of band at 19 000 cm^{-1} at rotational resolution,[18] (*b*) analysis of band at 16 000 cm^{-1} at rotational resolution.[19]

to the non-local corrections are neglected in these MIX calculations.

The Gaussian basis sets (GTOs) and the auxiliary basis sets needed for the Coulomb and exchange potential were optimized specifically for LSD calculations by Godbout *et al.*[33] For nickel, one GTO set of double-ζ quality was used with two contraction patterns, (63321/531*/41+) and (63321*5211*/41+) (using Huzinaga's notation[34]). It contains one d-diffuse and one p-polarization function. For oxygen, a double-ζ basis set with two contraction patterns, (621/41/1*) and (721/621/1*), and a triple-ζ basis set with the contraction pattern (7111/411/1*) were used. These sets both contain a d-polarization function. Calculations for each of the three approaches (VWN, BP and MIX) described above have been performed with each of the possible combinations of basis functions. All calculations were performed in an all-electron treatment. Vibrational frequencies were calculated by finite differentiation of analytic first derivatives. The symmetric stretch, the bending mode and the antisymmetric stretch of the linear $[NiO_2]^{2-/3-}$ ions are denoted ν_{sym}, ν_δ and ν_{asym} respectively. The stretch of the NiO molecule is denoted ν_{sym}.

The CLF model of Gerloch and Woolley[35-37] has been used successfully for many years to model the ligand-field properties of transition-metal complexes. The CLF calculations were performed on these systems using the CAMMAG 4 suite of programs.[38] The CLF parameters e_σ(O) and e_π(O) were used for the σ and π interactions between the transition metal and oxygen, the 'central' Racah parameters *B* and *C* for interelectron repulsion and ζ for spin–orbit coupling. The interpretation of e_σ(O) is discussed more fully below. The full d^8 basis of spin triplet and spin singlets was used for the nickel(II) compounds.

Results and Discussion

NiO

Table 1 lists the calculated Ni–O bond length and stretching frequency for the three levels of theory obtained using the less contracted nickel basis set and the triple-ζ set for oxygen for the ground state and several of the lowest-lying excited states. The calculations for the other combinations of basis sets gave similar results and are not presented here in the interests of brevity. The Ni–O bond length is found to be considerably more sensitive to the more or less contracted nature of the nickel p functions than to the quality of the oxygen basis set. This result was also observed by Bridgeman[15] for $NiCl_2$ and for $CuCl_2$ by Rogemond *et al.*[14] The best results for this open-shell system are found using the Vosko–Wilk–Nusair LSD approximation of the exchange-correlation potential, the less-contracted basis set for nickel and the triple-ζ basis set for chlorine. The Kohn–Sham eigenvalue diagram for this calculation is shown in Fig. 1. Starting from the ionic extreme of a $Ni^{2+}O^{2-}$ system, the relative σ-to-π charge donation by the oxide ions is roughly in the ratio 2:1.

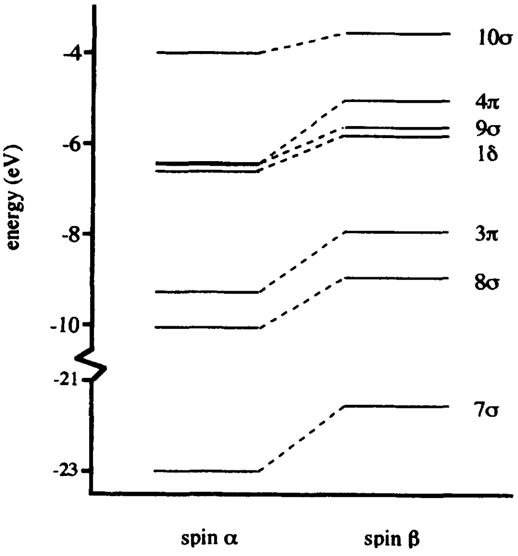

Fig. 1 Kohn–Sham eigenvalue diagram for the $^3\Sigma^-$ ground state of NiO

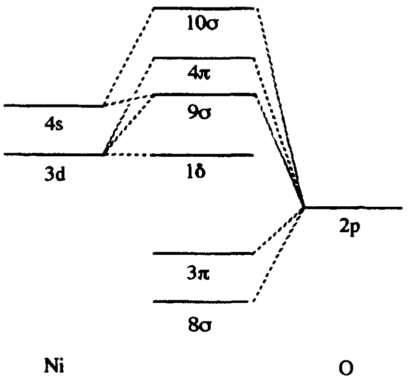

Fig. 2 Qualitative orbital diagram for the NiO molecule

The LDF calculations concur with the results of high-resolution spectral measurements of Srdanov and Harris[18] and Friedman-Hill and Field[19] in predicting a $^3\Sigma^-$ ground state. The dominant configuration is $(8\sigma)^2(3\pi)^4(1\delta)^4(9\sigma)^2(4\pi)^2$ to this state. Fig. 2 shows a qualitative orbital scheme for this system. The 8σ is a bonding orbital and is composed of nickel 4s, 3d$_\sigma$ and oxygen 2p$_\sigma$ functions. The 3π orbital is also bonding and is composed of nickel 3d$_\pi$ and oxygen 2p$_\pi$ functions. The 1δ orbitals are non-bonding and are completely Ni $3d_\delta$ in character. The 9σ orbital is antibonding and is composed mostly of Ni 4s and $3d_\sigma$. The 4π orbital is also antibonding and is composed of Ni $3d_\pi$ and O $2p_\pi$ functions. The 10σ orbital is unoccupied in the ground state. It is antibonding and is composed mostly of Ni 4s and $3d_\sigma$. The 10σ orbital is occupied in the $^3\Sigma^-$ excited state studied by Friedman-Hill and Field.[19] The $[16.0]^3\Sigma^-$–$X^3\Sigma^-$ and $[16.0]^3\Sigma^-$–$[4.3]^3\Pi_i$ transitions (where the energy of the state is given in square brackets preceding the state label) are predominantly 'd $\longleftrightarrow$ s' in character. The calculated energies of the $^3\Pi$ and $^3\Sigma^-$ excited states are in excellent agreement with the observed energies, as shown in Table 1. The calculated dipole moment is 3.93 D (1.31×10^{-29} C m). No experimental value appears to have been obtained for this molecule but the calculated dipole moment is in line with those obtained for other first-row transition-metal oxides.[39] It corresponds to $Ni^{\delta+}O^{\delta-}$ with the effective charge, $\delta = 0.46$.

The functions which are mostly d orbital in character are 1δ, 9σ and 4π and so the ligand-field splitting is in the order $d_\pi > d_\sigma > d_\delta$. Both the $3d_\sigma$ and 4s orbitals on nickel are able to overlap with the oxygen $2p_\sigma$ function. In high-oxidation-state transition-metal complexes the overlap with the metal 4s orbital appears to dominate[2] because of the radially contracted nature of the metal 3d functions. In cubic systems and in many high-co-ordinate systems where the metal d and s functions transform with different symmetries the d-orbital splitting is determined by the relative effectiveness of ligand σ and π donation. In tetragonally distorted octahedra, square-planar, linear molecules and in low-symmetry systems, however, the metal s orbitals and one or more of the d orbitals have the same symmetry and, as a result, may mix. In the present system the metal 4s and $3d_\sigma$ and the oxygen $2p_\sigma$ orbitals interact and three orbitals result: 8σ, 9σ and 10σ. The 8σ orbital is, as discussed above, bonding and is predominantly oxygen in character. The relatively similar energies of 9σ and 10σ in NiO results in significant mixing and this is enough to ensure that 9σ is lower in energy than 4π. The ligand-field splitting $d_\pi > d_\sigma > d_\delta$ does *not* imply greater π than σ donation from the oxygen ligand.

It is instructive to consider the ligand-field potential associated with the single oxide ligand in the NiO molecule. In AOM or CLF analyses of transition-metal complexes[36,40] the global ligand-field potential is divided up into a number of contributions from different 'local' cells, each cell usually being associated with one ligand. The NiO molecule appears to present a particularly simple case for such a treatment as only one cell is required and the local and global frames are identical. The AOM or CLF e_λ parameters are the exact energy shifts of the d_λ orbitals caused by the ligand field. The λ label represents the symmetry of the d orbitals in the local (and in this case also global) frame. In the CLF model[35–37] the ligand-field potential, V_{LF}, is dominated by the so-called 'dynamic' term, equation (1),

$$V_{LF} \approx \sum_{\chi} \frac{\mathscr{H}^{(1)}|\chi_\lambda\rangle\langle\chi_\lambda|\mathscr{H}^{(1)}}{\varepsilon_d - \tilde{\varepsilon}_\lambda} \qquad (1)$$

and the e_λ parameters are the matrix elements, $\langle d_\lambda|V_{LF}|d_\lambda\rangle$, of this operator in a pure d-orbital basis.

The χ orbitals in equation (1) have energy $\tilde{\varepsilon}_\lambda$ and are built from all the non-d orbitals in the molecule. The operator $\mathscr{H}^{(1)}$ is the aspherical part of the potential-energy operator V, where V is a function of the total molecular electron density minus that of the d electrons. The terms in the summation likely to be significant will be those where the χ functions are spatially and energetically close to the d orbitals. These functions are the bonding and low-lying antibonding orbitals in the molecule. The energy shifts of the d orbitals result from indirect interaction with the χ functions of appropriate symmetry according to the form of the potential (1). Non-zero e_λ parameters result only if there are bonding or low-lying antibonding χ orbitals of λ symmetry. The summation (1) allows for the possibility that there is more than one function with a particular symmetry. The energy shift of the d orbital is then the sum of the individual shifts caused by the functions. The denominator in equation (1) can be positive or negative and so the shifts can add together or subtract from each other.

The symmetry of the NiO molecule is $C_{\infty v}$ and so the λ labels required for the nickel d orbitals are σ, π and δ. The important χ orbitals are built from all the valence orbitals (except the nickel d orbitals): oxygen $2s_\sigma$, $2p_\sigma$ and $2p_\pi$ and nickel $4s_\sigma$, $4p_\sigma$ and $4p_\pi$. These valence orbitals overlap to form the bonding and antibonding χ orbitals. The e_σ parameter is thus the sum of four parts, equation (2), where $\chi_\sigma(1)$ and $\chi_\sigma(2)$ are bonding

$$e_\sigma = \sum_{i=1}^{4} \frac{\langle d_\sigma|\mathscr{H}^{(1)}|\chi_\sigma(i)\rangle\langle\chi_\sigma(i)|\mathscr{H}^{(1)}|d_\sigma\rangle}{\varepsilon_d - \tilde{\varepsilon}_\sigma(i)} \qquad (2)$$

orbitals and are composed mostly of oxygen $2s_\sigma$ and $2p_\sigma$ respectively. These are lower in energy than the d orbitals leading to a positive denominator and to positive terms in the summation; they are donor functions. Orbitals $\chi_\sigma(3)$ and $\chi_\sigma(3)$ are antibonding and are mostly nickel $4s_\sigma$ and $4p_\sigma$ in character. These are higher in energy than the d orbitals leading to a negative denominator and to negative terms in the summation; they are acceptor functions. The parameter thus becomes as in equation (3) where the orbital labels give an approximate

$$e_\sigma = e_\sigma(\mathrm{O}\ 2s_\sigma) + e_\sigma(\mathrm{O}\ 2p_\sigma) + e_\sigma(\mathrm{Ni}\ 4s_\sigma) + e_\sigma(\mathrm{Ni}\ 4p_\sigma) \qquad (3)$$

description of the character of the χ function. Similarly the e_π parameter is given by the sum of a positive and a negative term, equation (4), and e_δ the parameter is given by equation (5)

$$e_\pi = e_\pi(\mathrm{O}\ 2p_\pi) + e_\pi(\mathrm{Ni}\ 4p_\pi) \qquad (4)$$

$$e_\delta = 0 \qquad (5)$$

because of the lack of any δ orbitals in the molecule with suitable energy. The e_σ and e_π parameters obtained from an analysis of this system must then be interpreted according to the summations shown, the terms in which cannot be separated. Equations (3) and (4) can be approximated somewhat by neglecting the contribution from the oxygen 2s and nickel 4p orbital, as these lie very low and very high in energy respectively, so that expressions (6) and (7) are obtained. The e_σ parameter is thus

$$e_\sigma \approx e_\sigma(\mathrm{O}\ 2p_\sigma) + e_\sigma(\mathrm{Ni}\ 4s_\sigma) \qquad (6)$$

$$e_\pi \approx e_\pi(\mathrm{O}\ 2p_\pi) \qquad (7)$$

the sum of a positive term (accounting for the interaction between nickel $3d_\sigma$ and oxygen $2p_\sigma$) and a negative term (accounting for the mixing between nickel $3d_\sigma$ and $4s_\sigma$). Both of these are likely to be significant in magnitude. The resulting parameters could, in principle, be either positive or negative and could be larger or smaller than the value of e_π.

The $\chi_\sigma(2)$ function, as outlined above, is the bonding function formed predominantly by overlap of the oxygen $2p_\sigma$ and nickel $4s_\sigma$ orbitals and gives rise to the $e_\sigma(\mathrm{O}\ 2p_\sigma)$ term in equation (6). It is localized between the nickel and oxygen atoms. The $\chi_\sigma(3)$ function is the antibonding function formed predominantly by overlap of the oxygen $2p_\sigma$ and nickel $4s_\sigma$ orbitals and gives rise to the $e_\sigma(\mathrm{Ni}\ 4s_\sigma)$ term. It is localized away from the internuclear region. An alternative modelling of the ligand field in this molecule can be obtained by a decomposition of the potential into parts. This leads to the more conventional interpretation of ligand-field parameters. The first part, or cell, is localized in the nickel–oxygen internuclear region and gives rise to $e_\sigma(\mathrm{O})$ and $e_\pi(\mathrm{O})$ parameters where the oxygen $2p_\sigma$ and $2p_\pi$ functions are to be found. The second cell contains the rest of the molecule. This cell contains no ligands and is termed[35–37] a 'void' cell. The χ functions formed predominantly from the nickel 4s and 4p

Table 2 Calculated and observed transition energies (in cm^{-1}) in the ligand-field spectrum of NiO

State[a]	Strong-field configuration[a]	Ω	Energy/cm^{-1} calc.	Energy/cm^{-1} obs.[19]
$^1\Sigma_g^+$ (S)	$\delta_g{}^4\sigma_g{}^0\pi_g{}^4$	0+	46 229	—
$^1\Gamma_g$ (G)	$\delta_g{}^2\sigma_g{}^2\pi_g{}^4$	4	27 327	—
$^1\Delta_g$ (G)	$\delta_g{}^3\sigma_g{}^1\pi_g{}^4$	2	21 737	—
$^1\Sigma_g^+$ (G)	$\delta_g{}^2\sigma_g{}^2\pi_g{}^4$	0+	19 712	—
$^1\Phi_g$ (G)	$\delta_g{}^3\sigma_g{}^2\pi_g{}^3$	3	19 657	—
$^3\Sigma_g^-$ (P)	$\delta_g{}^2\sigma_g{}^2\pi_g{}^4$	1	18 886	—
		0+	18 533	
$^1\Pi_g$ (G)	$\delta_g{}^3\sigma_g{}^2\pi_g{}^3$	1	17 880	—
$^1\Sigma_g^+$ (D)	$\delta_g{}^4\sigma_g{}^2\pi_g{}^2$	0+	14 912	—
$^1\Pi_g$ (D)	$\delta_g{}^4\sigma_g{}^1\pi_g{}^3$	1	14 724	—
$^1\Delta_g$ (D)	$\delta_g{}^4\sigma_g{}^2\pi_g{}^2$	2	11 072	{12 500}[b]
$^3\Pi_g$ (P)	$\delta_g{}^3\sigma_g{}^2\pi_g{}^3$	1	10 732	—
		2	10 431	
		0−	10 374	
		0+	10 321	
$^3\Delta_g$ (F)	$\delta_g{}^3\sigma_g{}^1\pi_g{}^4$	1	10 048	—
		2	9 859	
		3	9 726	
$^3\Phi_g$ (F)	$\delta_g{}^3\sigma_g{}^2\pi_g{}^3$	2	7 595	
		3	6 988	
		4	6 363	{6 200}[b]
$^3\Pi_g$ (F)	$\delta_g{}^4\sigma_g{}^1\pi_g{}^3$	0+	4 583	4 700
		0−	4 512	—
		1	4 304	4 300
		2	3 991	3 900
$^3\Sigma_g^-$ (F)	$\delta_g{}^4\sigma_g{}^2\pi_g{}^2$	1	50	50
		0+	0	0

[a] Approximate descriptions. [b] Value from LDF calculations.

functions are to be found in this region. The presence of antibonding χ functions and the non-zero value of $\mathscr{H}^{(1)}$ in this cell leads to a non-zero ligand-field potential. The modelling of the ligand field by this decomposition must lead to the same result obtained above by the consideration of the molecule as a whole. It must be done with care. The number and position of void cells used must be chosen so that the global potential is completely but correctly modelled. In the present example the void cell can be taken to be a sphere with a cone containing the nickel–oxygen internuclear vector and the oxygen-localized functions removed. The parameters that result for this void cell are then as given in equations (8) and (9). If the nickel 4p functions are again neglected then the void leads to expressions (10) and (11).

$$e_\sigma(\text{void}) = e_\sigma(\text{Ni } 4s_\sigma) + e_\sigma(\text{Ni } 4p_\sigma) \tag{8}$$

$$e_\pi(\text{void}) = e_\sigma(\text{Ni } 4p_\pi) \tag{9}$$

$$e_\sigma(\text{void}) = e_\sigma(\text{Ni } 4s_\sigma) \tag{10}$$

$$e_\pi(\text{void}) = 0 \tag{11}$$

The physical basis for the use of void cells[41] and the neglect of e_π(void)[42] have recently been questioned and criticized. These criticisms have been addressed in detail.[37,43] The non-zero ligand-field potential in empty cells results from the presence there of antibonding functions of mostly metal s- and p-orbital character. The neglect of e_π(void) is paralleled within the AOM by the neglect of e_{dp} and results from the much larger energy difference between the metal d and p functions than between the d and s functions. The use of void cells is a way of modelling the global ligand-field potential whilst maintaining the extremely successful cellular scheme of the CLF model. The χ function composed predominantly of the metal s orbital is necessarily global in character and is difficult to localize. Its effect can either be treated globally or by using void cells in appropriate positions. Thus in square-planar molecules, for example, the ligand orbitals overlap with the metal s orbital to produce a bonding a_{1g} orbital localized in the metal–ligand internuclear regions and an antibonding a_{1g} orbital which maximizes away from the internuclear regions. Both of these orbitals lead to an energy shift of the global $d_{a_{1g}}$ orbital. The ligand-field potential resulting from the bonding orbital can be decomposed into cells associated with each ligand. That resulting from the antibonding orbital cannot be so easily modelled but void cells placed above and below the molecular plane where the orbital maximizes lead to an energy shift of the global $d_{a_{1g}}$ orbital and no effect on the other d orbitals as required by the global symmetry. The number and positioning of void cells is chosen so that all important sources of the global ligand-field potential are correctly modelled.

The spectrum of NiO is the least thoroughly investigated[18,19,39,44] of the first row transition-metal oxide molecules. The work of Srdanov and Harris[18] and of Friedman-Hill and Field[19] has established the $^3\Sigma^-$ symmetry of the ground state. The zero-field splitting and order has been determined with the $\Omega = 1$ component approximately 50 cm^{-1} above the $\Omega = 0$ level. The excited state at approximately 4300 cm^{-1} above the ground state is assigned[19] to $^3\Pi$ and the energies and identities of the $\Omega = 0+$, 1 and 2 spin–orbit levels have been determined. The rotational constant for this state is quite similar to that of the ground state and this is consistent with the $^3\Pi$ state being an excited ligand-field state. The upper levels at approximately 19 000 and 16 000 cm^{-1} studied by Srdanov and Harris and by Friedman-Hill and Field respectively have considerably smaller rotational constants than that of the ground state. The values are consistent with charge-transfer states.

The ligand-field analysis of NiO is thus limited to the measured positions and identities of the spin–orbit levels of the $^3\Sigma^-$ ground state and of the $^3\Pi$ excited state. In addition, the energies of a $^3\Phi$ and a $^1\Delta$ (the lowest-lying singlet) state were calculated by the LDF approach, as described above. The CLF analysis thus sought to reproduce the experimental results and to use the LDF results as a guide to the energies of the $^3\Phi$ and $^1\Delta$ states. The analysis required five parameters: the CLF parameters e_σ and e_π, the Racah interelectron repulsion parameters B and C and the spin–orbit coupling parameter ζ. As outlined above, the CLF parameters must be interpreted in terms of the summations shown in equations (6) and (7). The calculated energies of all the ligand-field states and their assignments are shown in Table 2. The agreement with the experimental energies is good and is of the quality usually obtainable using ligand-field calculations. The calculated energies also agree well with the LDF energies of the $^3\Phi$ and $^1\Delta$ states. The $^3\Pi$ state is predicted by the CLF calculations to be the lowest-lying excited state in agreement with the conclusions of Friedman-Hill and Field.[19] The ligand-field parameter values obtained are listed in Table 3. This table also includes the values obtained[47] for solid NiO. The most notable feature of the CLF analysis of the NiO molecule is the very large value for e_π, compared to the value estimated for NiO(s). This value is presumably a reflection of the considerably larger π donation and shorter bond length in the diatomic molecule. The sevenfold increase is even larger than the four-fold increase for e_π(Cl) observed between the $NiCl_2$ and $[NiCl_4]^{2-}$ systems.[15] The value of e_σ is much smaller than that of e_π. This result was also found for $NiCl_2$. The $e_\pi > e_\sigma$ relationship is necessary to obtain the $^3\Sigma^-$ ground state predicted by both experiment and theory. As outlined above, it does not imply that the π donation is more important than the σ donation. The value of e_σ is due to the combined effect of oxygen $2p_\sigma$ donation and nickel d–s mixing. These effects cannot be separated. If it is assumed that the latter term is similar to that the ≈6000 cm^{-1} stabilization in the energy of the $d_{a_{1g}}$ orbital observed[11] for the square-planar $[CuCl_4]^{2-}$ ion, the e_σ(O) term in e_σ is approximately equal to the value for

Table 3 The CLF parameter values (in cm^{-1}) and bond lengths for NiO(g), NiO(s), $[NiO_2]^{2-}$ and $NiCl_2$(g)

	e_σ(X)	e_π(X)	e_π(X)/e_σ(X)	Σ^a	*B*	*C*	ζ	Ref.	Ni–X/Å	Ref.
NiO(g)	4 460	7 680	1.7	19 820	320	4 375	450	*b*	1.626	19
$[NiO_2]^{2-}$	1 600	5 000	3.1	23 200	600	3 600	460	*b*	1.687	4
	6 500	3 500	0.54	27 000	729	3 920	460	17		
NiO(s)^c	4 300	1 075	0.25	38 700	600	—	—	43	2.10	45
$NiCl_2$	2 309	3 621	1.57	19 102	614	3 808	650	15	1.63	46

[a] $\Sigma = e_\sigma + e_\pi$ where the summation is over all ligands in the molecule. [b] This work. [c] e_σ and e_π obtained from Δ_{oct} assuming the relationship $e_\pi/e_\sigma = 0.25$ which is likely to be approximately correct for this octahedrally co-ordinated species.

Table 4 Calculated and experimentally determined properties of the ground states of the $[NiO_2]^{2-}$ and $[NiO_2]^{3-}$ ions

				Vibrational wavenumbers*/cm^{-1}		
		Bond length/Å	Bond angle/°	ν_{sym}	ν_δ	ν_{asym}
$[NiO_2]^{2-}$						
Calc.	VWN	1.687	180	776	186	891
	BP	1.714	180	653	206	840
	MIX	1.724	180	686	211	835
Exptl	refs. 3, 4, 16	1.687	180	732.5	—	—
$[NiO_2]^{3-}$						
Calc.	VWN	1.737	180	690	156	820
	BP	1.741	180	640	206	798
	MIX	1.759	180	635	189	790
Exptl	$KNa_2[NiO_2]$	1.790/1.771	175.0	668	—	829
	$K_3[NiO_2]$	1.759	176.9	673		837
	refs. 6, 16					

* The calculated values are all for the ^{58}Ni- and ^{16}O-containing isotope.

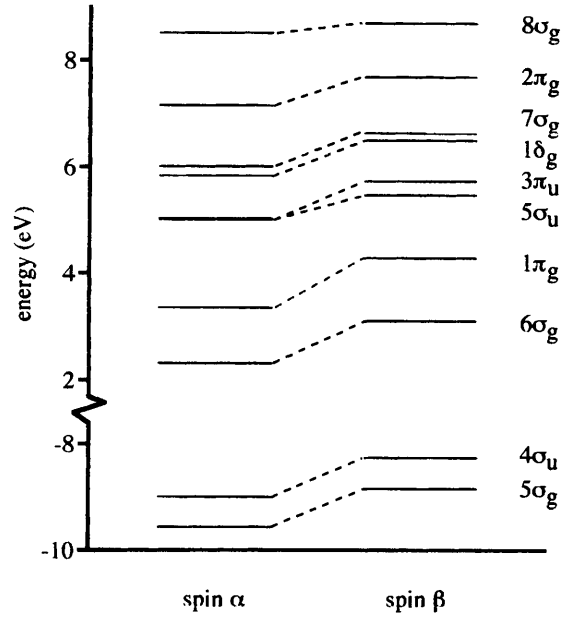

Fig. 3 Kohn–Sham eigenvalue diagram for the $^3\Sigma_g^-$ ground state of the linear $[NiO_2]^{2-}$ ion

e_π(O). A e_σ(O):e_π(O) ratio in line with the LDF prediction of greater σ than π donation requires a greater d–s effect in NiO. This may result from a smaller energy difference between the antibonding function of predominantly metal s-orbital character and the d orbitals in NiO than in the higher-co-ordinate $[CuCl_4]^{2-}$ system.

$[NiO_2]^{2-}$ ion

Table 4 lists the calculated Ni–O bond length and vibrational frequencies for the three levels of theory obtained using the less-contracted nickel basis set and the triple-ζ set for oxygen for the ground state. The calculations for the other combinations of basis sets gave similar results and are not presented here in the interests of brevity. The best results for this open-shell system are again found using the Vosko–Wilk–Nusair LSD approximation of the exchange-correlation potential, the less-contracted basis set for nickel and the triple-ζ basis set for chlorine. The Kohn–Sham eigenvalue diagram for this calculation is shown in Fig. 3. The positive energies result from performing the calculations on the negatively charged ion. The positive crystal field experienced by the ion in the solid state stabilizes the energy levels but although this effect is considerable the relative energies should remain unaffected.[48] Starting from the ionic extreme of a Ni^{2+} and O^{2-} system, the relative σ-to-π charge donation by the oxide ions is roughly in the ratio 2:1, similar to that in NiO but there is less overall donation from each oxide.

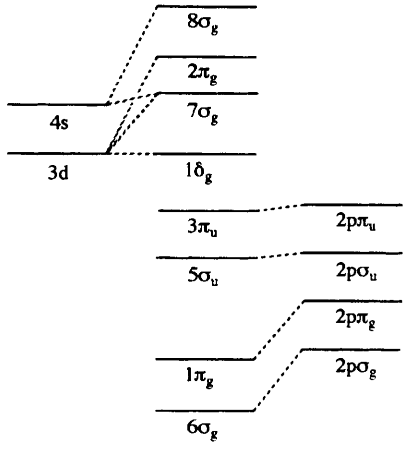

Fig. 4 Qualitative orbital diagram for linear $[NiO_2]^{n-}$ ions

The LDF calculations predict a $^3\Sigma_g^-$ ground state. Fig. 4 shows a qualitative orbital scheme for a linear NiO_2 system.

Table 5 Calculated and observed transition energies (in cm^{-1}) in the ligand-field spectrum of $K_2[NiO_2]$

State*	Strong-field configuration*	Energy/cm^{-1}		
		Ω	calc.	obs.[17]
$^1\Sigma_g^+$ (S)	$\delta_g^4\sigma_g^0\pi_g^4$	0+	50 631	—
$^1\Gamma_g$ (G)	$\delta_g^2\sigma_g^2\pi_g^4$	4	33 199	—
$^1\Delta_g$ (G)	$\delta_g^3\sigma_g^1\pi_g^4$	2	27 894	—
$^3\Sigma_g^-$ (P)	$\delta_g^2\sigma_g^2\pi_g^4$	0+	26 666	—
		1	26 516	
$^1\Sigma_g^+$ (g)	$\delta_g^2\sigma_g^2\pi_g^4$	0+	25 399	—
$^1\Phi_g$ (G)	$\delta_g^3\sigma_g^2\pi_g^3$	3	23 213	—
$^1\Pi_g$ (G)	$\delta_g^3\sigma_g^2\pi_g^3$	1	20 988	19 950, 19 310
$^1\Pi_g$ (D)	$\delta_g^4\sigma_g^1\pi_g^3$	1	18 261	18 630, 17 990
$^1\Sigma_g^+$ (D)	$\delta_g^4\sigma_g^2\pi_g^2$	0+	17 108	17 360
$^3\Pi_g$ (P)	$\delta_g^3\sigma_g^2\pi_g^3$	0−	16 385	16 710
		0+	16 085	16 160
		1	16 035	
		2	15 974	
$^3\Delta_g$ (F)	$\delta_g^3\sigma_g^1\pi_g^4$	1	15 937	15 590
		2	15 603	
		3	15 137	
$^1\Delta_g$ (D)	$\delta_g^4\sigma_g^2\pi_g^2$	2	11 263	11 275
$^3\Phi_g$ (F)	$\delta_g^3\sigma_g^2\pi_g^3$	2	9 317	9 780
		3	8 761	9 050
		4	8 092	8 420, 8 040
$^3\Pi_g$ (F)	$\delta_g^4\sigma_g^1\pi_g^3$	0+	7 504	7 470
		0−	7 456	7 325
		1	7 219	7 100
		2	6 992	
$^3\Sigma_g^-$ (F)	$\delta_g^4\sigma_g^2\pi_g^2$	1	37	—
		0+	0	0

* Approximate descriptions.

The dominant configuration to the $^3\Sigma_g^-$ ground state is $(6\sigma_g)^2(1\pi_g)^4(5\sigma_u)^2(3\pi_u)^4(1\delta_g)^4(7\sigma_g)^2(2\pi_g)^2$ outside the core of nickel $1s^22s^22p^6$ and oxygen $1s^22s^2$ electrons. The lowest-lying excited states are predicted to be $^3\Pi_g$ arising from the configuration $(1\delta_g)^4(7\sigma_g)^1(2\pi_g)^3$, $^3\Phi_g$ arising from $(1\delta_g)^3(7\sigma_g)^2(2\pi_g)^3$ and $^1\Delta_g$ arising from the configuration $(1\delta_g)^4(7\sigma_g)^2(2\pi_g)^2$. These states are calculated to be approximately 8500, 9600 and 10 100 cm^{-1} respectively above the $^3\Sigma_g^-$ ground state. The $1\delta_g$, $7\sigma_g$ and $2\pi_g$ orbitals are composed mainly of the nickel d orbitals and so the ligand-field splitting is again in the order $d_\pi > d_\sigma > d_\delta$. Just as in the NiO system described above, this energy sequence results from the interaction between the $7\sigma_g$ and $8\sigma_g$ orbitals which are mainly nickel $3d_\sigma$ and 4s in character. The ligand-field splitting does not imply greater π than σ donation from the oxygen atoms to the metal.

The treatment of the d–s mixing in a ligand-field analysis of a linear MX_2 system is very similar to that outlined above for the NiO system. Indeed one consequence of holohedral symmetry[49] when using a pure d-orbital basis is that the ligand-field potential arising from the two centrosymmetrically related ligands in MX_2 is indistinguishable from the potential arising from a single ligand with twice the ligand-field strength. Within the CLF scheme the global potential in a linear MX_2 is correctly modelled using two cells containing the X ligands and a third, cylindrically symmetric, 'void' cell perpendicular to the molecular axis. This modelling is detailed more thoroughly in the recent description of the ligand-field analyses of the $NiCl_2$ and $CuCl_2$ molecules.[15] The cylindrically symmetric void cell ensures that only the global d_σ orbital is shifted in energy. No e_π(void) parameter is required in this system because there are no antibonding orbitals of π_g symmetry and appropriate energy. The energies of the d orbitals are then as in equations (12). As only e_σ(O) and e_σ(void) affect the d_σ orbital, it is impossible to separate their effects and it is more appropriate to define a composite parameter, equation (13), and equation (12a) then simplifies to (12d).

$$\varepsilon(d_\sigma) = 2\,e_{\sigma'}(\mathrm{O}) + 2\,e_\sigma(\mathrm{void}) \qquad (12a)$$

$$\varepsilon(d_\pi) = 2\,e_\pi(\mathrm{Cl}) \qquad (12b)$$

$$\varepsilon(d_\delta) = 0 \qquad (12c)$$

$$e_\sigma(\mathrm{O}) = e_{\sigma'}(\mathrm{O}) + e_\sigma(\mathrm{void}) \qquad (13)$$

$$\varepsilon(d_\sigma) = 2\,e_\sigma(\mathrm{O}) \qquad (12d)$$

Hitchman *et al.*[17] have published a polarized absorption spectrum of the $[NiO_2]^{2-}$ ion in $K_2[NiO_2]$ and Rieck and Hoppe[3] have published magnetic data for this ion in a number of complexes. The spectrum consists of two broad bands at ≈9000 and at ≈16 000 cm^{-1} with the higher-energy band strongly polarized parallel to the O–Ni–O vector. Each band is structured and there are a number of weak features. The experimental magnetic moment, $\mu \approx 3.0\,\mu_B$, is found[3] to obey the Curie–Weiss law and so to be essentially independent of temperature in the range 70–295 K. Hitchman *et al.*[17] also reported AOM calculations but assumed a $^3\Pi$ ground state, based on the ligand-field splitting $d_\sigma > d_\pi > d_\delta$. In view of the LDF results, the spectrum and magnetism have been reanalysed assuming a $^3\Sigma_g^-$ ground state.

The calculated ligand-field transition energies are listed and assigned in Table 5. Very good agreement with the experimental spectrum is found using the optimum CLF parameter set given in Table 3, although it should be noted that no transition is calculated near the extremely weak feature in the spectrum at *ca.* 13 500 cm^{-1}. The two strong bands in absorption spectrum at ≈9000 and at ≈16 000 cm^{-1} are reassigned as $\{^3\Phi_g, {}^3\Pi_g\} \longleftarrow {}^3\Sigma_g^-$ and $\{^3\Delta_g, {}^3\Pi_g\} \longleftarrow {}^3\Sigma_g^-$ respectively. The higher-energy band is observed to be strongly polarized parallel to the O–Ni–O axis. Its intensity is likely to be dominated by the $^3\Pi_g \longleftarrow {}^3\Sigma_g^-$ component as the $^3\Delta_g \longleftarrow {}^3\Sigma_g^-$ transition involves the two-electron jump $\delta_g^4\sigma_g^2\pi_g^2 \longrightarrow \delta_g^3\sigma_g^1\pi_g^4$. As the $[NiO_2]^{2-}$ unit is centrosymmetric, the Laporte-forbidden transitions occur only *via* vibronic coupling with the *ungerade* π_u bending and σ_u^+ asymmetric stretching vibrational modes. The

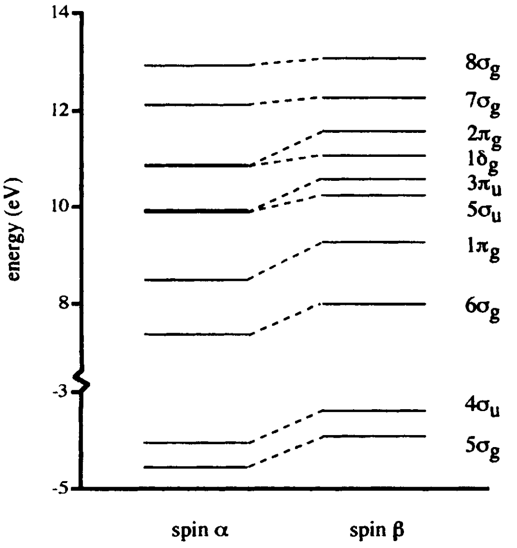

Fig. 5 Kohn–Sham eigenvalue diagram for the $^3\Sigma_g^-$ ground state of the linear $[NiO_2]^{3-}$ ion

$^3\Pi_g \longleftarrow {}^3\Sigma_g^-$ transition involves the orbital excitation $\delta_g{}^4\sigma_g{}^2\pi_g{}^2 \longrightarrow \delta_g{}^3\sigma_g{}^2\pi_g{}^3$. This transition is allowed parallel to the O–Ni–O axis due to coupling with the π_u bend and perpendicular to the O–Ni–O axis due to coupling with the σ_u^+ asymmetric stretch. The LDF calculations predict that the bending mode has a much lower frequency than that of the asymmetric stretch (see Table 4). Extensive experimental and theoretical studies[50] on $[CuCl_4]^{2-}$ suggest that soft bending modes are much more efficient generators of intensity than are stretches. If this is also true in the $[NiO_2]^{2-}$ ion, then it would lead to the $^3\Pi_g \longleftarrow {}^3\Sigma_g^-$ transition being strongly polarized parallel to the O–Ni–O axis, as observed.

The experimental magnetic moment $\mu \approx 3.0\ \mu_B$ and very weak temperature dependence strongly suggests an orbitally non-degenerate, spin-triplet ground state, in agreement with the LDF calculations. Using the CLF parameters obtained above to reproduce the absorption spectrum, the calculated magnetic moment for the $^3\Sigma_g^-$ ground state is $\mu_{295\,K} \approx 3.1\ \mu_B$ with an orbital-reduction factor in line with the expected covalency of the complex, $k = 0.7$. The relatively small calculated zero-field splitting of the $^3\Sigma_g^-$ ground state and relatively large energy of the first excited state (see Table 5) lead to a small temperature dependence in agreement with the experimental measurements. The orbitally degenerate $^3\Pi$ ground state assumed by Hitchman *et al.*[17] however gives $\mu_{295\,K} \approx 3.5\ \mu_B$ using $k = 0.7$ and the observed magnetic moment is only reproduced if the orbital contribution is almost completely quenched by using $k = 0.3$. The relatively large first-order spin–orbit splitting of the $^3\Pi$ ground term and low energy of the first excited state however lead to a significant temperature dependence, with $\mu_{70\,K} \approx 2.7\ \mu_B$ and $\mu_{295\,K} \approx 3.0\ \mu_B$, even using this very small k parameter. The magnetic behaviour is much more satisfactorily reproduced if a $^3\Sigma_g^-$ ground state is assumed.

$[NiO_2]^{3-}$ ion

Table 4 lists the calculated Ni–O bond length and vibrational frequencies for the three levels of theory obtained using the less-contracted nickel basis set and the triple-ζ set for oxygen for the ground state. The calculations for the other combinations of basis sets gave similar results and are not presented here in the interests of brevity. The Kohn–Sham eigenvalue diagram for the VWN calculation is shown in Fig. 5. Starting from the ionic extreme of a Ni^+ and O^- system, the relative σ-to-π charge donation by the oxide ions is roughly in the ratio 1.3 : 1, somewhat smaller than that in NiO and in the $[NiO_2]^{2-}$ ion. The LDF calculations predict that the $[NiO_2]^{3-}$ ion is linear. Crystallographic studies[6,16] of the ion in $KNa_2[NiO_2]$ and $K_3[NiO_2]$ show small departures from linearity. The LDF calculations predict a small barrier to bending and this is revealed by the softness of the bending vibrational mode (see Table 4). Fig. 6 shows how the energy of the system changes and the Ni–O bond lengthens as the O–Ni–O angle is decreased from 180°. For small changes from linearity the energy only increases very slightly and so lattice effects, as discussed by Möller *et al.*,[16] probably lead to the bent geometry.

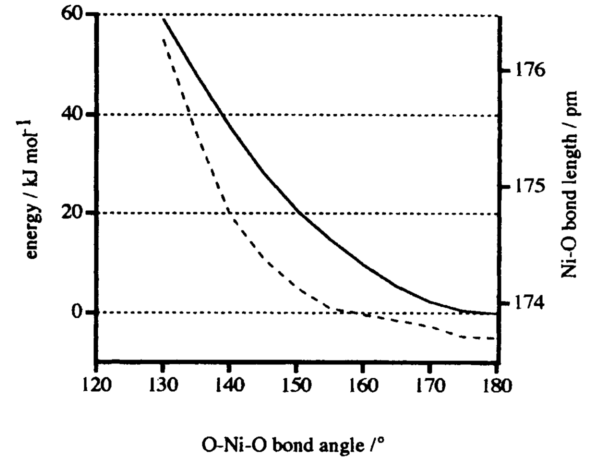

Fig. 6 Energy (solid line) and Ni–O bond length (dashed line) as a function of the bond angle in the $[NiO_2]^{3-}$ ion

The LDF calculations predict a $^2\Sigma_g^+$ ground state. The dominant configuration to the $^2\Sigma_g^+$ ground state is $(6\sigma_g)^2(1\pi_g)^4(5\sigma_u)^2(3\pi_u)^4(1\delta_g)^4(2\pi_g)^4(7\sigma_g)^1$ outside the core of nickel $1s^22s^22p^6$ and oxygen $1s^22s^2$ electrons. As discussed by Möller *et al.*,[16] the EPR g values for this complex strongly suggest a $^2\Sigma_g^+$ ground state with the unpaired electron localized largely in the nickel d_σ orbital. The LDF calculations are consistent with this interpretation of the EPR spectrum although the $7\sigma_g$ orbital is predicted to be almost equally 4s and d_σ in character.

The lowest-lying excited states are predicted to be $^2\Sigma_g^+$ arising from the configuration $(1\delta_g)^4(2\pi_g)^4(7\sigma_g)^1(8\sigma_g)^1$, A $^2\Pi_g$ from $(1\delta_g)^4(2\pi_g)^3(7\sigma_g)^1(8\sigma_g)^1$, B $^2\Pi_g$ from $(1\delta_g)^4(2\pi_g)^3(7\sigma_g)^2$ and $^2\Delta_g$ from $(1\delta_g)^3(2\pi_g)^4(7\sigma_g)^2$. These states are calculated to be approximately 1000, 6500, 11 000 and 15 100 cm^{-1} respectively above the $^2\Sigma_g^+$ ground state. The absorption spectra of $K_3[NiO_2]$ and $KNa_2[NiO_2]$ have also been recorded by Möller *et al.*[16] Bands are observed at *ca.* 6000 and 12 000 cm^{-1}. These are assigned, on the basis of the LDF calculations, as the A $^2\Pi_g \longleftarrow {}^2\Sigma_g^+$ and B $^2\Pi_g \longleftarrow {}^2\Sigma_g^+$ transitions respectively. The electron excitation involved in both of these transitions causes an increase in the occupation of antibonding σ_g orbitals. This is consistent with the decrease in the frequency of ν_{sym} compared to the value in the ground state reported by Möller *et al.*[16] The relatively low energy of the A $^2\Pi_g$ state may lead to extensive spin–orbit coupling with the $^2\Sigma_g^+$ ground state resulting in the significant observed $g_\perp$ shift in the EPR spectrum. The A $^2\Pi_g \longleftarrow {}^2\Sigma_g^+$ transition involves promotion from $2\pi_g$ to $8\sigma_g$. This transition certainly cannot be characterized as a 'd–d' excitation and so a CLF (or AOM) calculation is not suitable. Owing to their greater radial expansion in the +1 oxidation state, there is much more involvement of the nickel 3d orbitals in this complex and it is unlikely that ligand-field theory is appropriate for the study of this system.

Möller *et al.*[16] reported AOM calculations using the assignments $^2\Pi_g \longleftarrow {}^2\Sigma_g^+$ and $^2\Delta_g \longleftarrow {}^2\Sigma_g^+$ for the low- and high-energy spectral transitions respectively. They were able to reproduce the transition energies and the g values. The calculation of the latter required a very large orbital reduction factor, $k = 0.96$, which, as the authors point out, seems unreasonable as far as a simple ligand-field description of the bonding is concerned. The calculation of two transition energies required only two parameters for this d^9 system which are effectively orbital energy differences. The reproduction of the spectrum therefore does not demonstrate the applicability of ligand-field theory to this system. The magnetic behaviour, however, requires much more accurate wavefunctions and it is possible that the inability to reproduce the absorption and EPR spectra simultaneously using parameters within normally acceptable limits is an indication of the failure of ligand-field theory. It is important that calculations using semiempirical models such as the CLF and AOM should be able to reproduce, simultaneously, all experimental measurements.[51]

Conclusion

LCGTO-LDF calculations on NiO and on the $[NiO_2]^{2-}$ and $[NiO_2]^{3-}$ ions have been reported. Nickel oxide is predicted to have a $^3\Sigma^-$ ground state, in agreement with recent experimental and theoretical studies; $[NiO_2]^{2-}$ is predicted to be linear and to have a $^3\Sigma_g^-$ ground state in contrast to a previous study[17] which assumed a $^3\Pi$ ground state. The CLF calculations are able to reproduce very satisfactorily the absorption spectrum and magnetic behaviour of this ion assuming a $^3\Sigma_g^-$ ground state. In both NiO and $[NiO_2]^{2-}$ the d-orbital splitting required to produce the predicted ground states is $d_\pi > d_\sigma > d_\delta$, in contrast to that predicted by qualitative crystal-field arguments and simple molecular orbital considerations. This d-orbital energy sequence was also predicted[15] for the $NiCl_2$ molecule which is isoelectronic with the $[NiO_2]^{2-}$ ion.

This sequence results from strong π donation from the ligand and considerable mixing between orbitals of predominantly d_σ and metal 4s character. Such mixing is an important feature of the electronic structure of non-cubic systems and its modelling is a key aspect of the ligand-field study[37] of such systems. The global nature of the ligand-field potential arising from orbitals of predominantly metal s-orbital character must be very carefully implemented[15] in local ligand-field models such as the CLF or the AOM. Within the CLF scheme the effect is implemented using 'void' cells. Although these do not contain ligands there is a non-zero ligand field associated with them because they are placed where the global orbital of predominantly metal s character maximizes.

Linear and square-planar complexes may be considered to be the limiting cases produced by tetragonal distortion of octahedral complexes. In square-planar systems this mixing results in the $d_{a_{1g}}$ orbital being significantly stabilized. The resulting gap between $d_{a_{1g}}$ and the lowest unoccupied orbital ensures that d^8 square-planar complexes are almost universally low spin and hence diamagnetic. In linear complexes, such as those studied here, the mixing stabilizes d_σ. This mixing appears to be sufficient[12–15] in $CuCl_2$, $NiCl_2$, NiO and $[NiO_2]^{2-}$ to push d_σ below d_π resulting in ground states which differ from those predicted by simple crystal-field considerations. The somewhat similar energies of the d_σ and d_π orbitals in these systems results from the enhanced π bonding compared to that in higher-coordinate systems and from the 'd–s' mixing. It ensures that these linear systems are high spin and paramagnetic.

The bonding in $[NiO_2]^{3-}$ is less straightforward because of the similar energy and size of the metal s and d orbitals and both are involved extensively in the bonding. The lower oxidation state of the metal and the presence of an extra antibonding electron results in less donation from the oxide ligand and weaker bonding. The description of transitions as 'd–d' excitations is inappropriate and a modelling of the spectral and magnetic behaviour using ligand-field theory is probably unsuitable.

Acknowledgements

The author would like to thank Dr. Malcolm Gerloch of the University of Cambridge for the use of the CAMMAG 4 program suite and Dr. Alain St-Amant of the University of Ottawa for making the DEFT code publicly available.

References

1 P. A. Cox, *Transition Metal Oxides*, Clarendon Press, Oxford, 1995.
2 M. Gerloch and E. C. Constable, *Transition Metal Chemistry*, VCH, Weinheim, 1994.
3 V. H. Rieck and R. Hoppe, *Z. Anorg. Allg. Chem.*, 1973, **400**, 311.
4 B. Nowitzki and R. Hoppe, *Croat. Chem. Acta*, 1984, **57**, 537.
5 W. Burrow, J. Birx, F. Bernhardt and R. Hoppe, *Z. Anorg. Allg. Chem.*, 1993, **619**, 923.
6 F. Bernhardt and R. Hoppe, *Z. Anorg. Allg. Chem.*, 1993, **619**, 969.
7 C. W. DeKock and D. M. Gruen, *J. Chem. Phys.*, 1966, **44**, 4387.
8 C. W. DeKock and D. M. Gruen, *J. Chem. Phys.*, 1967, **46**, 1096.
9 A. B. P. Lever and B. R. Hollebone, *Inorg. Chem.*, 1972, **11**, 2183.
10 D. W. Smith, *Inorg. Chim. Acta*, 1971, **5**, 231.
11 D. W. Smith, *Inorg. Chim. Acta*, 1977, **22**, 107.
12 C. W. Bauschlicher, jun. and B. O. Roos, *J. Chem. Phys.*, 1989, **91**, 4785.
13 R. J. Deeth, *J. Chem. Soc., Dalton Trans.*, 1993, 1061.
14 F. Rogemond, H. Chermette and D. R. Salahub, *Chem. Phys. Lett.*, 1994, **219**, 228.
15 A. J. Bridgeman, *J. Chem. Soc., Dalton Trans.*, 1996, 2601.
16 A. Möller, M. A. Hitchman, E. Krausz and R. Hoppe, *Inorg. Chem.*, 1995, **34**, 2684.
17 M. A. Hitchman, H. Stratemeier and R. Hoppe, *Inorg Chem.*, 1988, **27**, 2506.
18 V. I. Srdanov and D. O. Harris, *J. Chem. Phys.*, 1988, **89**, 2748.
19 E. J. Friedman-Hill and R. W. Field, *J. Mol. Spectrosc.*, 1992, **155**, 259.
20 S. P. Walch and W. A. Goddard, *J. Am. Chem. Soc.*, 1978, **100**, 1338.
21 M. Dolg, U. Wedig, H. Stoll and H. Preuss, *J. Chem. Phys.*, 1987, **86**, 2123.
22 C. W. Bauschlicher, jun., *Chem. Phys.*, 1985, **93**, 399.
23 C. W. Bauschlicher, jun., C. J. Nelin and P. S. Bagus, *J. Chem. Phys.*, 1985, **82**, 3265.
24 C. W. Bauschlicher, jun. and P. Maitre, *Theor. Chim. Acta*, 1995, **90**, 189.
25 *Local Density Approximations in Quantum Chemistry and Solid-State Physics*, eds. J. P. Dahl and J. Avery, Plenum, New York, 1989.
26 R. G. Parr and W. Yang, *Density-Functional Theory of Atoms and Molecules*, Oxford University Press, Oxford, 1989.
27 *Density Functional Methods in Chemistry*, eds. J. K. Labanowski and J. W. Andelm, Springer, New York, 1991.
28 T. Ziegler, *Chem. Rev.*, 1991, **91**, 651.
29 A. St-Amant, DEFT, a FORTRAN program, University of Ottawa, 1994.
30 S. H. Vosko, L. Wilk and M. Nusair, *Can. J. Phys.*, 1980, **58**, 1200.
31 A. D. Becke, *Phys. Rev. A*, 1988, **38**, 3098.
32 J. P. Perdew, *Phys. Rev. B*, 1986, **33**, 8822.
33 N. Godbout, D. R. Salahub, J. Andzelm and E. Wimmer, *Can. J. Chem.*, 1992, **70**, 1992.
34 *Gaussian Basis Sets for Molecular Calculations*, ed. S. Huzinaga, Elsevier, New York, 1984.
35 M. Gerloch, J. H. Harding and R. G. Woolley, *Struct. Bonding (Berlin)*, 1981, **46**, 1.
36 M. Gerloch, *Magnetism and Ligand-Field Analysis*, Cambridge University Press, Cambridge, 1984.
37 A. J. Bridgeman and M. Gerloch, *Prog. Inorg. Chem.*, in the press.
38 CAMMAG 4, a FORTRAN program, A. R. Dale, M. J. Duer, N. D. Fenton, M. Gerloch and R. F. McMeeking, University of Cambridge, 1996.
39 A. J. Merer, *Annu. Rev. Phys. Chem.*, 1989, **40**, 407.
40 C. E. Schäffer, *Struct. Bonding (Berlin)*, 1968, **5**, 68.
41 C. E. Schäffer, *Inorg. Chim. Acta*, 1995, **240**, 581.
42 J. I. Zink, *J. Chem. Soc., Dalton Trans.*, 1996, 4027.
43 A. J. Bridgeman and M. Gerloch, *J. Chem. Soc., Dalton Trans.*, 1996, 4027.
44 L. Malet and B. Rosen, *Bull. Soc. R. Sci. Liege*, 1945, **14**, 382.
45 H. Krebs, *Fundamentals of Inorganic Crystal Chemistry*, McGraw-Hill, London, 1968.
46 S. H. Ashworth, F. J. Grieman, J. M. Brown, P. J. Jones and I. R. Beattie, *J. Am. Chem. Soc.*, 1993, **115**, 2978.
47 C. K. Jørgensen, *Adv. Chem. Phys.*, 1963, **5**, 33.
48 H. Johansen and N. K. Anderson, *Mol. Phys.*, 1986, **58**, 965.
49 C. K. Jørgensen, *Modern Aspects of Ligand-field Theory*, North-Holland, Amsterdam, 1971.
50 A. J. Bridgeman and M. Gerloch, *Inorg. Chem.*, 1995, **34**, 4370.
51 A. J. Bridgeman and M. Gerloch, *Chem. Phys. Lett.*, 1995, **247**, 304.

Received 5th July 1996; *Paper* 6/04711D